0026-895X/06/7002-718–726$20.00
MOLECULAR PHARMACOLOGY
Copyright © 2006 The American Society for Pharmacology and Experimental Therapeutics
Mol Pharmacol 70:718–726, 2006

Vol. 70, No. 2
23473/3128275
Printed in U.S.A.

State-Dependent Verapamil Block of the Cloned Human $Ca_v3.1$ T-Type Ca^{2+} Channel

Benjamin S. Freeze, Megan M. McNulty, and Dorothy A. Hanck

Department of Medicine, Section of Cardiology, University of Chicago, Chicago, Illinois

Received February 16, 2006; accepted May 12, 2006

ABSTRACT

Verapamil is a potent phenylalkylamine antihypertensive believed to exert its therapeutic effect primarily by blocking high-voltage-activated L-type calcium channels. It was the first clinically used calcium channel blocker and remains in clinical use, although it has been eclipsed by other calcium channel blockers because of its short half-life and interactions with other channels. In addition to blocking L-type channels, it has been reported to block T-type (low-voltage activated) calcium channels. This type of cross-reactivity is likely to be beneficial in the effective control of blood pressure. Although the interactions of T channels with a number of drugs have been described, the mechanisms by which these agents modulate channel activity are largely unknown. Most calcium channel blockers exhibit state-dependence (i.e., preferential binding to certain channel conformations), but little is known about state-dependent verapamil block of T channels. We stably expressed human $Ca_v3.1$ T-type channels in human embryonic kidney 293 cells and studied the state-dependence of the drug with macroscopic and gating currents. Verapamil blocked currents at micromolar concentrations at polarized potentials similar to those reported for L-type channels, although unlike for L-type currents, it did not affect current time course. The drug exhibited use-dependence and significantly slowed the apparent recovery from inactivation. Current inhibition was dependent on potential. This dependence was restricted to negative potentials, although all data were consistent with verapamil binding in the pore. Gating currents were unaffected by verapamil. We propose that verapamil achieves its inhibitory effect via occlusion of the channel pore associated with an open/inactivated conformation of the channel.

T-type, or low-voltage-activated, calcium channels are characterized by a low threshold of activation, a small unitary conductance, and slow deactivation (Fox et al., 1987a,b; Perez-Reyes, 2003). T channels can be blocked or otherwise modulated by multiple classes of drugs, including antiepileptics, antihypertensives, and anesthetics (Heady et al., 2001). Verapamil is a clinically used phenylalkylamine antihypertensive that is believed to be somewhat selective for L-type calcium channels in native tissues, with estimated IC_{50} values ranging from 600 nM in vascular smooth muscle (Kuga et al., 1990) to 3 μM in ventricular myocytes (Nawrath and Wegener, 1997). However, the much greater IC_{50} values of 40.5 μM (Dilmac et al., 2004) and 120 μM (Motoike et al., 1999) reported for L-type channels in heterologous expression systems suggest that the actual affinities in vivo may be somewhat lower. Verapamil has also been shown to block T channels, with IC_{50} values of 30 μM in vascular smooth muscle (Kuga et al., 1990) and 70 μM in spermatogenic cells (Arnoult et al., 1998). T channels, like L channels, seem to be blocked in a state-dependent manner (Nawrath and Wegener, 1997; Motoike et al., 1999; Heady et al., 2001; Dilmac et al., 2004). Because T-channel blockade has been implicated in the reduction of vascular tone in vitro (Boulanger et al., 1994; Karila-Cohen et al., 1996; Lam et al., 1998; VanBavel et al., 2002; Jensen et al., 2004), the interactions of verapamil with this channel may prove to be therapeutically relevant.

Selective stabilization of an inactivated state is the most widely accepted explanation of how verapamil inhibits currents in L-type channels. Block of L-type current is accompanied by prominent use-dependence, slowing of recovery kinetics, and shift of the steady-state inactivation curve to hyperpolarized potentials (Nawrath and Wegener, 1997; Dilmac et al., 2004). Multiple pore-lining residues of the L-type channel have been implicated in phenylalkylamine binding (Hockerman et al., 1995, 1997; Johnson et al., 1996; Motoike

This work was supported by Howard Hughes Undergraduate Research Fellowships (to B.S.F.), an American Heart Association Predoctoral Fellowship (to M.M.M.), and by National Institutes of Health grant R01-HL65680 (to D.A.H.).

This work was published in part in abstract form: Freeze BS, McNulty MM, and Hanck DA (2004) Verapamil block of human T-type Ca^{2+} channels. *Biophys J* **86:**426a.

Article, publication date, and citation information can be found at http://molpharm.aspetjournals.org.

doi:10.1124/mol.106.023473.

ABBREVIATIONS: HEK, human embryonic kidney; BAPTA, 1,2-bis(2-aminophenoxy)ethane-*N*,*N*,*N*′,*N*′-tetraacetic acid; MES, 2-(*N*-morpholino)-ethanesulfonic acid; ANOVA, analysis of variance; Q-V, charge-voltage.

et al., 1999; Dilmac et al., 2004), suggesting that the high-affinity binding site is located in the pore.

As is the case for many T-channel blockers, the detailed process by which verapamil inhibits T-channel currents is not known. In the present study, we sought to elucidate the mechanism by which verapamil blocks the T-type calcium channel. We expressed a common splice variant of the human $Ca_v3.1$ T-type channel in HEK-293 cells and examined the effects of verapamil on macroscopic and gating currents. The drug blocked macroscopic currents at micromolar concentrations but did not affect current time course. Verapamil slowed recovery from inactivation and blocked current in a use- and holding potential-dependent fashion. The drug competed with the permeant ion, suggesting that it bound in the pore. However, block was unaffected by the current-eliciting potential. $Ca_V3.1$ gating currents were also unaltered in the presence of verapamil, suggesting that the drug does not affect normal gating of the channel, despite its ability to inhibit ionic currents. This finding and our macroscopic data strongly suggest that verapamil inhibits currents by occlusion of the conduction pathway in open and inactivated conformations of the channel.

Materials and Methods

Heterologous Expression. The cDNA of a $Ca_v3.1$ splice variant (217) was kindly provided by M. C. Emerick and W. S. Agnew (The Johns Hopkins University School of Medicine, Baltimore, MD) and subcloned into pcDNA3.1/Zeocin for transfection into HEK-293 cells and pcDNA5/FRT/TO for transfection into Flp-In T-REx-293 cells (Invitrogen, Carlsbad, CA). Stable cell lines were created using either 200 μg/ml Zeocin (for HEK-293 cells) or 100 μg/ml hygromycin (for T-REx-293 cells). Cells were maintained in Dulbecco's modified Eagle's medium (Invitrogen) in 100-mm Corning culture dishes supplemented with 10% fetal bovine serum, 1% penicillin-streptomycin, and either 100 μg/ml Zeocin (for HEK-293 cells) or 1% L-glutamine, 15 μg/ml blasticidin, and 50 μg/ml hygromycin (for T-REx-293 cells). $Ca_V3.1$ expression in T-REx-293 cells was induced with 10 μg/ml tetracycline ~18 h before use in electrophysiology experiments. Similar results were obtained for both cell lines.

Solutions and Chemicals. Bath solutions for ionic current experiments contained 2 mM $CaCl_2$, 140 mM NaCl, and 10 mM HEPES, and were titrated to pH 7.4 with 1 N NaOH. The pH 7.4 pipette solution contained 130 mM NaCl, 10 mM HEPES, 5 mM MgATP, 1 mM $CaCl_2$, and 11 mM EGTA, titrated to pH 7.4 with 1 N NaOH. For experiments at pH 6.1, HEPES was reduced to 5 mM, EGTA was reduced to 1 mM, and 5 mM MES was added to the solution. In some experiments, the pipette solution additionally contained 500 μM sodium-BAPTA, which improved seal resistances. The addition of sodium-BAPTA had no effect on channel properties. The gating current bath solution contained 140 mM *N*-methyl-D-glucamine, 10 mM HEPES, 2 mM $CaCl_2$, and 2 mM $MgCl_2$, pH 7.4, with HCl. $LaCl_3$ (500 μM) was freshly added to bath solution to block ionic currents. The pipette solution contained 140 mM *N*-methyl-D-glucamine, 10 mM HEPES, 10 mM EGTA, 1 mM $CaCl_2$, and 5 mM magnesium-ATP, pH 7.4, with HCl. Verapamil (Sigma, St. Louis, MO) solutions were made fresh daily by preparing and diluting a 1 mM aqueous solution into bath solution to achieve the desired concentration.

Electrophysiological Recordings and Analysis. All experiments were performed on trypsinized cells (0.25% Trypsin-EDTA; Invitrogen) 2 to 6 days after plating. Whole-cell ionic current voltage-clamp recordings were made using pCLAMP 8 software and Axopatch-1D or Axopatch-200B feedback amplifiers with Digidata 1320A or 1322A interfaces (Molecular Devices, Sunnyvale, CA). Patch pipettes were pulled with a P97 micropipette puller (Sutter Instruments, Novato, CA) from TW 150-4 borosilicate (World Precision Instruments, Sarasota, FL) or Garner 8250 (Garner Glass Co., Claremont, CA) glass capillary tubes, and had resistances of 1.0 to 2.5 MΩ when filled with pipette solution. Data were filtered at 5 kHz by an eight-pole low-pass Bessel filter and digitized at 10 to 20 kHz. Recordings were made at room temperature (20–26°C). Currents were additionally filtered at 1 kHz offline. Drug was applied to a single chamber bath in which solutions were exchanged using the cFLOW perfusion system (Cell Microcontrols, Virginia Beach, VA) or the SF77 Perfusion Fast-Step system (Warner Instruments, Hamden, CT). Both methods of drug application yielded similar steady-state results.

Gating currents were recorded in whole-cell mode using an Axopatch 200B feedback amplifier with a National Instruments digital-to-analog converter and LabView 7.0 data acquisition software (National Instruments Corporation, Austin, TX). Patch pipettes were pulled with a P97 micropipette puller (Sutter Instruments) from TW 150-4 borosilicate glass capillary tubes (World Precision Instruments) and had resistances of 1.0 to 4.0 MΩ when filled with pipette solution. Data were filtered at 10 kHz using an eight-pole low-pass Bessel filter and sampled at 50 kHz. Four repetitions of each voltage step were performed ¼ of 60 Hz out of phase and averaged to increase the signal-to-noise ratio. Linear capacitative currents were subtracted from the current measurements using 40-mV hyperpolarizing steps to voltages at which no gating charge was expected to move (−120 to −160 mV). The gating currents were integrated to determine gating charge.

Curve-fitting and statistical analyses (Student's *t* test, ANOVA) were performed using Matlab (The Mathworks, Inc., Natick, MA) and Origin software (OriginLab Corp., Northampton, MA). Data are depicted as mean ± S.E.M. * denotes $p < 0.05$, ** denotes $p < 0.01$, and *** denotes $p < 0.001$. For second statistical comparisons, † denotes $p < 0.05$ and ‡ denotes $p < 0.01$.

Results

Verapamil Affinity for Cloned T-Type and L-Type Channels Is Comparable. We studied the splice variant of $Ca_V3.1$ that is most abundantly expressed in adult human brain. It differs from the original clone (Perez-Reyes et al., 1998) in that it is human and includes one additional exon (14), a short segment in the domain I to II linker. It is electrophysiologically similar to the clone without exon 14 (proteins paper, in press). By expressing this channel in a heterologous system, we were able to determine verapamil affinity with minimal interference by other conductances. We estimated a lower bound for verapamil affinity by measuring the inhibition of peak currents under conditions in which channels were fully available at the holding potential, fully activated at the current-eliciting potential, and the duration between consecutive pulses was long. Channels depolarized from −130 to −10 mV at a frequency of 0.2 Hz exhibited an IC_{50} of 21.4 μM, a value less than the affinities of 40.5 and 120 μM reported for low-frequency stimulation of L-type channels in heterologous systems (Motoike et al., 1999; Dilmac et al., 2004) and similar to the values previously reported for T channels in native tissues (Kuga et al., 1990; Arnoult et al., 1998). The experimental data were fit well by a single-site binding curve, suggesting that drug binding was not a cooperative process (Fig. 1). Although verapamil has been reported to speed the decay of L-type currents (Hockerman et al., 1995, 1997; Johnson et al., 1996; Nawrath and Wegener, 1997; Motoike et al., 1999; Dilmac et al., 2004), it did not affect the T-channel current time course.

Block Was Use-Dependent. Many calcium channel blockers more effectively inhibit currents when channels are depolarized at high frequencies as a result of enhanced access to high-affinity binding states. It has been reported that verapamil exhibits such use-dependent block of T channels (Arnoult et al., 1998) in mouse spermatogenic cells but not in rat aortic smooth muscle cells (Kuga et al., 1990). To assess whether verapamil blocks the cloned channel in a use-dependent fashion, we subjected cells to trains of 100-ms steps to −10 mV interspersed by variable duration hyperpolarizations to −130 mV (Fig. 2). Verapamil (10 μM) blocked ~25% of the peak current when channels recovered for either 9900 or 4900 ms between consecutive depolarizations. When the recovery interval was reduced to 400 ms, block significantly increased to 51%, and verapamil blocked 69% of the peak current when channels were allowed to recover for only 100 ms between depolarizations. The prominent use-dependence of block indicated that verapamil preferentially bound to channel states entered upon membrane depolarization.

Verapamil Slowed Recovery from Fast Inactivation. The use-dependence of verapamil block suggested that the drug would slow the apparent rate of recovery from fast inactivation as well. We applied dual 50-ms pulses to −10 mV separated by variable duration steps to −130 mV to quantify the effect of verapamil on recovery kinetics. As expected, verapamil slowed recovery from fast inactivation in a dose-dependent manner (Fig. 3). In the absence of drug (control), the time course of recovery was well described by a biexponential function (Hering et al., 2004) with time constants of τ_{Fast} = 52 ms and τ_{Slow} = 233 ms. Upon the addition of 10 μM verapamil, τ_{Fast} increased only slightly to 87 ms, whereas τ_{Slow} increased 7-fold to 1671 ms (Fig. 3, inset). When the drug concentration was increased from 10 to 50 μM, there were no significant changes in the values of the exponential time constants. However, the amplitude of the slow component significantly increased, and the amplitude of the fast component significantly decreased, reflecting the increased proportion of drug-bound channels (Fig. 3, inset).

Affinity Increased with Holding Potential. Under 0.2 Hz depolarization to −10 mV, equilibrium inhibition of peak current by 10 μM verapamil significantly increased with holding potential. IC_{50} values calculated from the Langmuir adsorption isotherm decreased approximately linearly with potential, reaching a value of 4.9 μM at −70 mV (Fig. 4A). Because steady-state inactivation increased with holding potential as well, this finding implied that the drug targeted an inactivated state of the channel. However, because channels were exposed to drug throughout the activation, inactivation, and recovery processes, we could not rule out the possibility

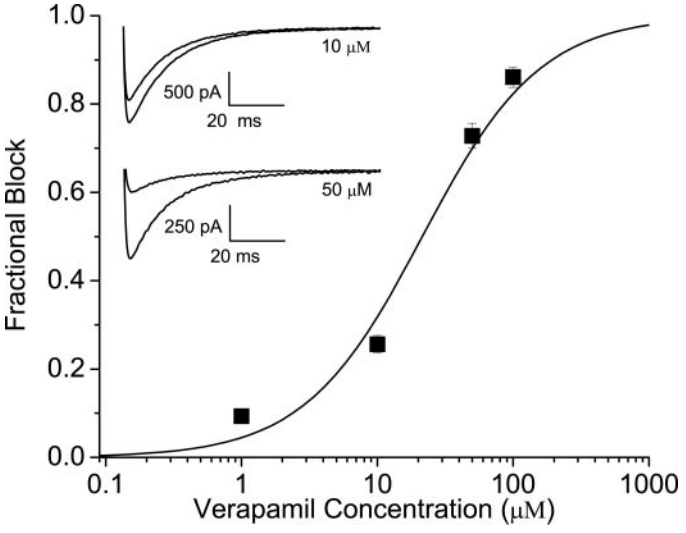

Fig. 1. Verapamil inhibits current at micromolar concentrations. Single-site binding curve (IC_{50} = 21.4 μM) generated under conditions of 0.2-Hz depolarization to −10 mV from a holding potential of −130 mV. A single drug concentration was tested on each cell to avoid issues with cumulative doses (1 μM, n = 2; 10 μM, n = 4; 50 μM, n = 3; 100 μM, n = 3). Inset, representative currents in the absence and presence of 10 or 50 μM verapamil. Verapamil reduced peak current but did not alter the current time course.

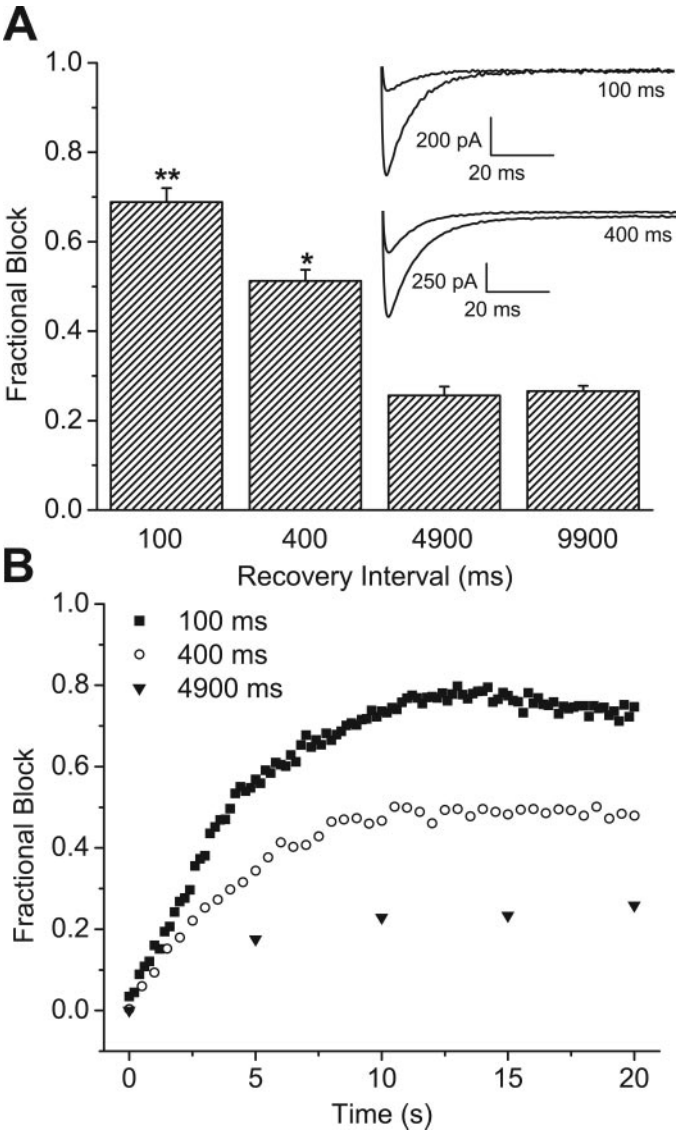

Fig. 2. Block was use-dependent. A, fractional block by 10 μM verapamil significantly increased as the interval between repetitive 100-ms depolarizations from −130 to −10 mV decreased (9900 ms, n = 2; 4900 ms, n = 4; 400 ms, n = 2; 100 ms, n = 3). Determinations of statistical significance were made compared with the fractional block in the protocol with a recovery interval of 9900 ms. Inset, representative currents in the absence and presence of 10 μM verapamil. Currents recorded with recovery intervals of 400 and 100 ms are depicted. B, representative block kinetics by 10 μM verapamil for recovery intervals of 100, 400, and 4900 ms. Fractional block was calculated by normalizing currents in drug to steady-state currents in the absence of drug.

that enhanced block at positive potentials instead resulted from preferential binding to some other state.

To assess whether the holding potential effect resulted mainly from drug binding to inactivated channels, we used a fast perfusion system to selectively administer 10 μM verapamil to inactivated channels. A 200-ms conditioning pulse was applied to inactivate channels in the absence of drug, followed by ~800-ms application of 10 μM verapamil at the conditioning potential. Cells were then removed from drug and repolarized to −130 mV for 100 ms, an interval sufficient to recover a large fraction of unblocked but not blocked channels (Fig. 3). A subsequent 50-ms step to −10 mV served as an assay for the remaining current. In the absence of drug, the fractional availability of channels under these recording conditions (Fig. 4B) decreased with conditioning potential at negative voltages and reached a plateau at voltages positive to −70 mV. When the fast perfusion system was used to precisely control drug application (Fig. 4C) during the voltage protocol, verapamil more potently blocked channels at depolarized potentials, with fractional block (Fig. 4D) tracking very tightly with channel availability (Fig. 4B). This finding strongly suggested that the voltage-dependence of verapamil inhibition under these conditions (~1 s inactivation time) and under steady-state conditions (~5 s inactivation time) was due primarily to differential drug access to high-affinity-inactivated states of the channel.

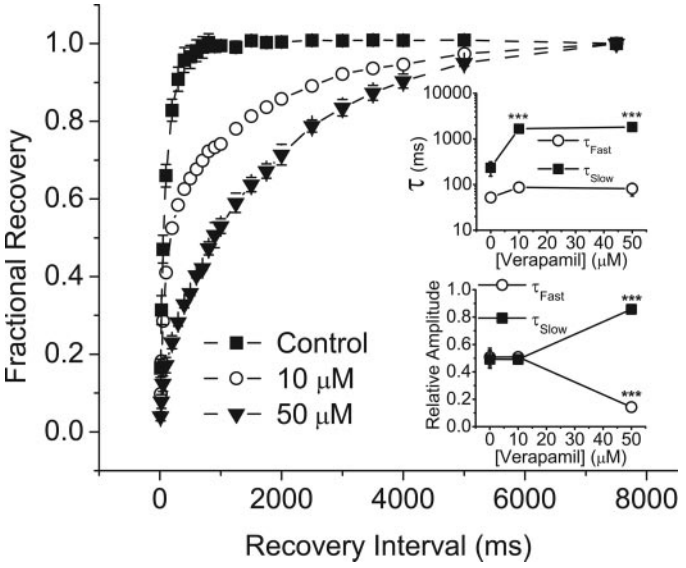

Fig. 3. Verapamil significantly slowed recovery from inactivation. Time course of recovery in the absence of verapamil (■) and in the presence of 10 μM (○) or 50 μM verapamil (▼) (control, $n = 5$; 10 μM, $n = 3$; 50 μM, $n = 2$). An initial 50-ms pulse to −10 mV inactivated channels and was followed by a variable duration recovery interval at −130 mV (the length of which increased from shortest to longest during the protocol) and a second 50-ms step to −10 mV to assay for remaining current. After each application of the dual-pulse protocol, membranes were hyperpolarized to −130 mV for 8 s to allow for maximal recovery before the next inactivating prepulse. Fractional recovery was calculated by normalizing to the current elicited by the final voltage pulse in the protocol. Top, inset, time constants produced from biexponential fits of the recovery kinetics. τ_{Fast} represents the fast component of a biexponential function, whereas τ_{Slow} is the time constant of the slower exponential component. Verapamil significantly increased τ_{Slow} by ~7-fold compared with the value in the absence of drug ($p < 0.001$) but did not significantly alter τ_{Fast} from the control value. Neither τ_{Fast} nor τ_{Slow} was significantly different across verapamil concentrations ($p > 0.05$). Bottom, inset, relative amplitudes of the exponential components. The relative amplitude of the fast component significantly decreased, and the relative amplitude of the slow component significantly increased when the verapamil concentration was increased from 10 to 50 μM.

Verapamil Did Not Target the Fast-Inactivated State During Short Depolarizations. Because verapamil binding to inactivated states was substantial during prolonged depolarization, we sought to determine whether inactivated state binding was a major contributor to inhibition on the time scale of the current. To this end, we exposed cells to trains of depolarizations from −130 to −10 mV, for which the time at −130 mV was held constant at 200 ms across all experimental conditions, and the time at −10 mV was varied from 6 to 50 ms. A 6-ms step resulted in a small proportion (~10%) of channels entering the inactivated state. The proportion of channels that inactivated increased as the step duration was lengthened; a 50-ms step inactivated nearly the entire population of channels. We expected that if verapamil selectively stabilized the fast-inactivated state of the channel, the degree of block would increase with the proportion of channels entering the state during depolarization. However, one-way ANOVA indicated that there were no significant differences in the fractional block of current across step durations (Fig. 5), demonstrating that access to the fast-inactivated state was unimportant in verapamil binding when channels were depolarized for such short durations.

Verapamil Interacted with the Permeant Ion. It has been reported that verapamil accesses its binding site from the intracellular space and binds in the pore of both L-type Ca^{2+} channels and K^+ channels (DeCoursey, 1995; Johnson et al., 1996; Robe and Grissmer, 2000; Dilmac et al., 2004). We hypothesized that verapamil would also bind in the pore of the T channel and predicted that it would compete with the permeant ion for a binding site. In the presence of 0.5 mM extracellular Ca^{2+}, 10 μM verapamil blocked 35% of the peak current under 0.2 Hz stimulation (Fig. 6). Consistent with our prediction, increasing the Ca^{2+} concentration to 2 mM significantly reduced block to 26%. In 5 mM Ca^{2+}, block was not significantly different from the value at 2 mM, indicating that verapamil only effectively competed with Ca^{2+} at relatively low Ca^{2+} concentrations.

The drug also more effectively competed with Ba^{2+} than with Ca^{2+} for a binding site. Verapamil (10 μM) blocked 42% of peak current in 2 mM Ba^{2+}, which was significantly greater than the 26% block observed in 2 mM Ca^{2+}. Block was significantly reduced to 24% at 5 mM Ba^{2+}. As was the case with Ca^{2+}, the competitive effect seemed to saturate at relatively low concentrations of Ba^{2+}: in 10 mM Ba^{2+}, block was not statistically different from the value at 5 mM.

Block Was Voltage-Independent. At intracellular pH 7.4, ~94% of verapamil molecules bear a positive charge because of protonation of their tertiary amino groups (pK_a 8.6; Budavari, 1996). Therefore, we expected that if verapamil bound at a pore site within the transmembrane field, block would depend on the voltage of the current-eliciting depolarization. We evaluated this hypothesis by depolarizing cells at 0.2 Hz from −130 mV to a wide range of potentials in the presence and absence of 10 μM verapamil. Under control conditions, the activation curve was described by a single Boltzmann function with a halfpoint of −57 mV and slope factor of e-fold/4.9 mV. We were surprised to find that the activation curve was unaffected by drug (10 μM verapamil: $V_{1/2}$ = −59 mV, slope factor = e-fold/5.5 mV; 50 μM vera-

pamil: $V_{1/2}$ = −56 mV, slope factor = e-fold/5.2 mV), indicating that block was a voltage-independent process (Fig. 7A).

Given this result, we hypothesized that use-dependent block would be voltage-independent as well. To test this, we used a voltage protocol consisting of 100-ms steps to either −10 or +80 mV, followed by 100-ms repolarizations to −130 mV. As predicted, the fractional block of current by 10 μM verapamil was unaffected by the current-eliciting voltage-step (68 ± 3% inhibition at −10 mV, 58 ± 3% inhibition at +80 mV; $p > 0.05$) (Fig. 7B), despite the 90-mV difference in membrane potential.

The Active Form of Verapamil Was Uncharged. The voltage-independence of block was initially puzzling because of the large proportion of charged drug molecules and the probable location of the binding site within the pore of the channel. We reasoned that either the binding site was outside of the transmembrane field or that the neutral form of the drug was mainly responsible for its inhibitory effect. To test the latter hypothesis, we lowered intracellular pH from 7.4 to 6.1. We calculated that the resultant pH gradient from cytoplasmic space to bath caused an approximately 20-fold increase in the intracellular concentration of charged drug, relative to the concentration at intracellular pH 7.4. Therefore, if charged verapamil was the primary active species of drug, block at acidic pH should have been as much as 20-fold greater than block at pH 7.4. Inconsistent with this hypothesis, verapamil blocked 45% of peak current under 0.2 Hz stimulation, less than 2-fold greater than the 26% block observed at intracellular pH 7.4. The moderate increase in fractional block compared with pH 7.4 suggests that the charged form may make a relatively minor contribution to the inhibitory effects of verapamil or that titration of ionizable channel residues increases affinity for the drug. Use-dependent block was not substantially altered either: under 5-Hz stimulation, verapamil blocked 72% of peak current, a value very similar to the 68% block at pH 7.4 (Fig. 8B).

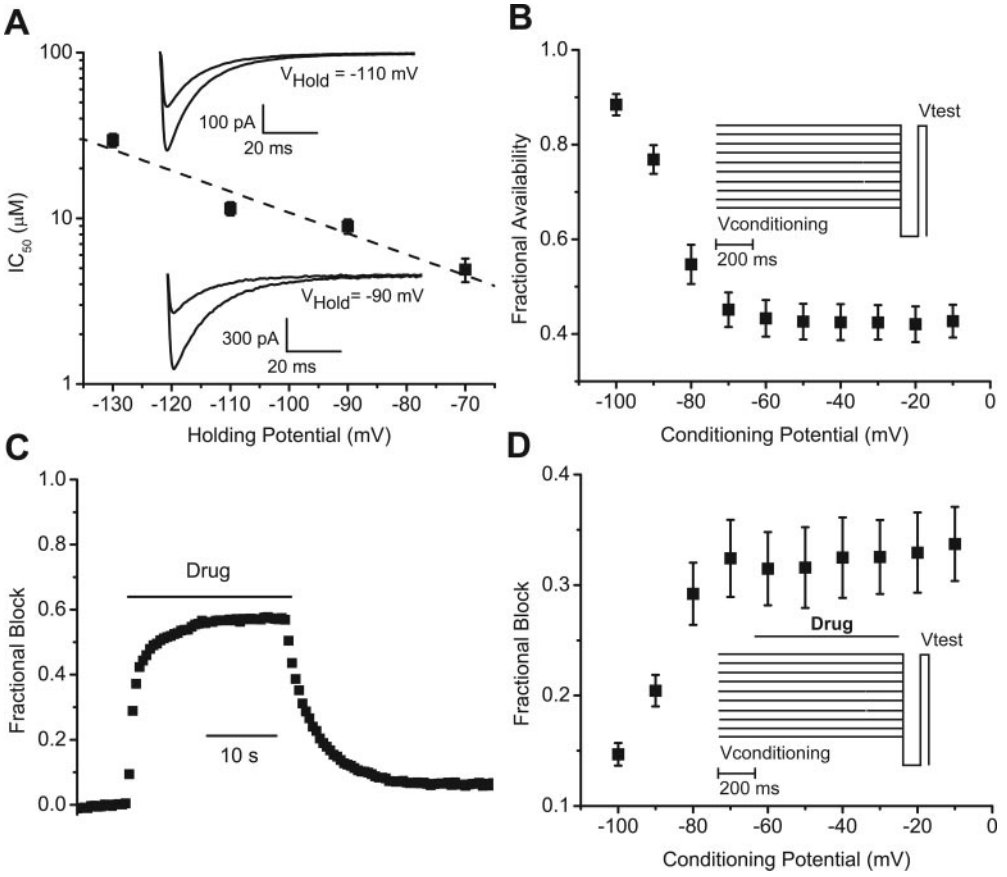

Fig. 4. Verapamil affinity increased with holding potential. A, the calculated verapamil IC_{50} value decreased nearly linearly with holding potential. Currents were elicited in the presence and absence of 10 μM verapamil by pulsing repetitively to −10 mV for 100 ms and allowing channels to recover for 4900 ms at the holding potential (−130 mV, n = 4; −110 mV, n = 3; −90 mV, n = 4; −70 mV, n = 2). Inset, representative currents for holding potentials of −110 and −90 mV. B, availability curve obtained in the absence of verapamil with the voltage protocol shown (inset). Cells were depolarized for 1 s at various potentials to promote inactivation. They were subsequently hyperpolarized to −130 mV for 100 ms and depolarized to −10 mV for 50 ms to measure the remaining current. These currents were normalized to control currents elicited under conditions of maximal availability (50-ms steps to −10 mV from a holding potential of −130 mV; data not shown). C, representative drug wash-on and wash-off kinetics using a fast perfusion system (also used in D) to expose channels to either control solution or 10 μM verapamil. This cell was repetitively depolarized to −10 mV for 100 ms and hyperpolarized to −130 mV for 400 ms between depolarizing steps. Because perfusion kinetics were very rapid, precise temporal control of drug application was possible in D. D, the holding potential dependence of drug block remained when inactivated channels were selectively exposed to 10 μM verapamil (n = 4). For each conditioning potential, the voltage protocol in B was first applied in the absence of drug. To determine the fractional block of current at that potential, the inset voltage protocol was then applied. Drug exposure commenced after the initial 200-ms interval at the conditioning potential and terminated just before the repolarization of the membrane to −130 mV. Fractional block at each potential was calculated by normalizing the current elicited by the V_{test} pulse in the presence of verapamil to the current elicited by V_{test} in the absence of drug. The duration between consecutive prepulses was ~4 s to allow for full channel recovery. Wash-off kinetics between prepulses were more rapid than in C, and cumulative drug effects did not occur. The voltage dependence of fractional block closely resembles the voltage dependence of channel availability in B.

Together, these findings strongly suggested that the uncharged molecule was the main inhibitory species of the drug. Furthermore, the activation curve was unshifted by 10 μM verapamil (control: $V_{1/2}$ = −64 mV, slope factor = e-fold/4.4 mV; 10 μM verapamil: $V_{1/2}$ = −65 mV, e-fold/4.4 mV), indicating that block remained a voltage-independent process at this pH (Fig. 8A). Although it is possible that the verapamil binding site is outside of the transmembrane field, the fact that the active form of the drug is uncharged implies that block would be voltage-independent regardless of binding site location.

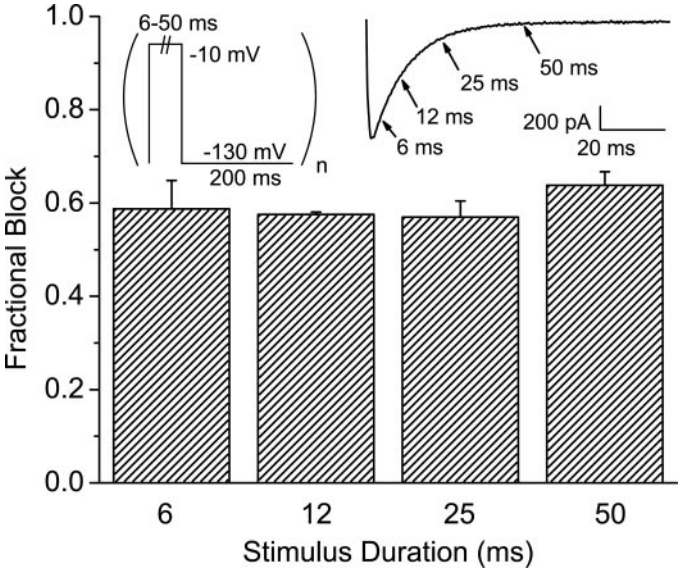

Fig. 5. Verapamil did not target the fast-inactivated state during short depolarizations. The fractional block of current by 10 μM verapamil for stimulus durations ranging from 6 to 50 ms with a constant recovery interval of 200 ms. Channels were opened by steps to −10 mV and recovered at −130 mV. The stimulus duration had no significant effect (by one-way ANOVA) on the steady-state magnitude of block, indicating that verapamil did not rely on access to the fast-inactivated state to inhibit currents during short voltage steps (6 ms, n = 2; 12 ms, n = 2; 25 ms, n = 2; 50 ms, n = 3). Left inset, voltage protocol used in this experiment. The number of depolarizations in the train was sufficient to achieve steady-state inhibition of current. Right inset, representative current trace in the absence of verapamil. The proportion of inactivated channels increased with longer stimulus durations.

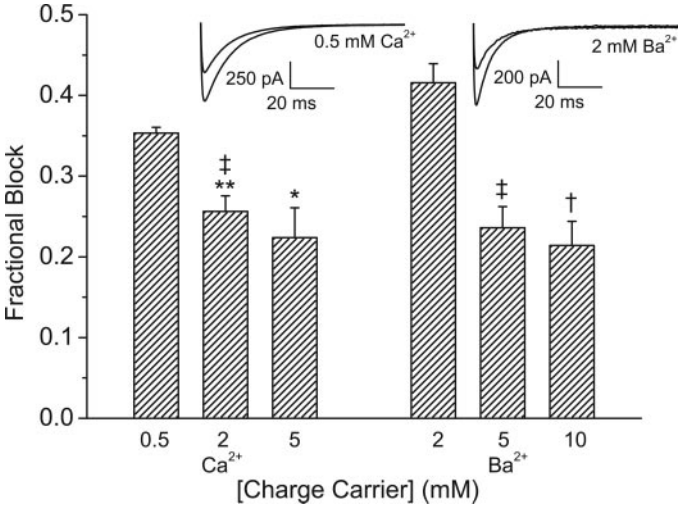

Fig. 6. Verapamil interacted with the divalent charge carrier. Block by 10 μM verapamil decreased with both Ca^{2+} and Ba^{2+} concentrations under 0.2 Hz stimulation. The competitive effect saturated at relatively low concentrations for both species of divalent. Determinations of statistical significance were made in comparison with either 0.5 mM Ca^{2+} (∗) or 2 mM Ba^{2+} (†) (0.5 mM Ca^{2+}, n = 3; 2 mM Ca^{2+}, n = 4; 5 mM Ca^{2+}, n = 3; 2 mM Ba^{2+}, n = 4; 5 mM Ba^{2+}, n = 3; 10 mM Ba^{2+}, n = 4). Inset, representative currents in the presence and absence of 10 μM verapamil recorded in either 0.5 mM Ca^{2+} or 2 mM Ba^{2+}.

Channels Gated Normally In the Presence of Drug. Given the ability of verapamil to effectively inhibit ionic currents, we wanted to determine whether the drug could also modulate voltage sensor movement. Many drug classes, including dihydropyridines (Hadley and Lederer, 1995) and local anesthetics (Sheets and Hanck, 2003), alter the movement of the gating charge in their target channels, an effect that probably contributes to their inhibitory properties. To test whether verapamil altered charge transfer, we measured ON-gating currents and charge in the presence of 500 μM La^{3+} to block ionic current. Cells were held at −120 mV and depolarized for 75 ms over a large voltage range (−120 to +80 mV) to elicit ON-gating currents. Figure 9, inset, shows

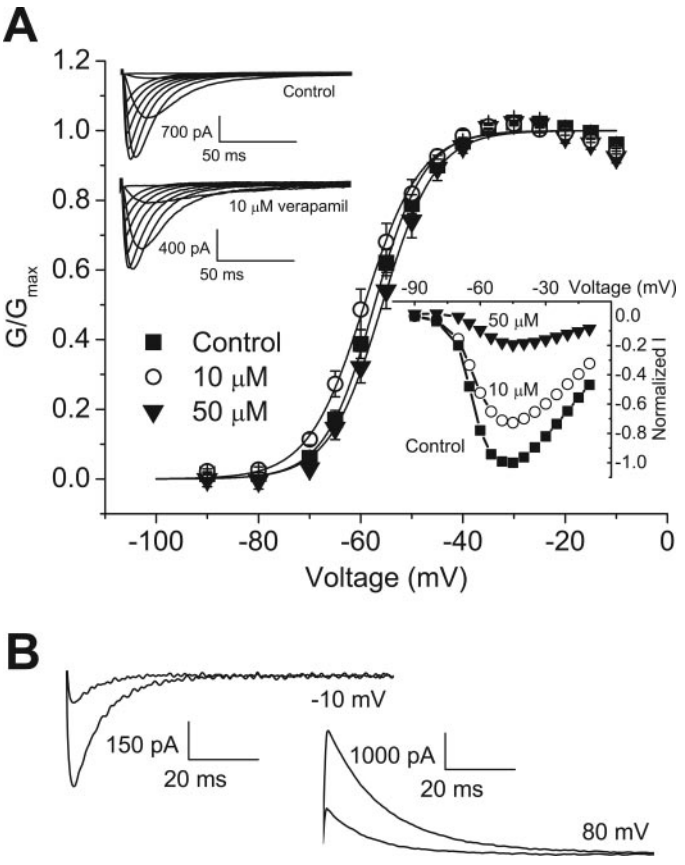

Fig. 7. Block was voltage-independent. A, activation curves produced from 200-ms depolarizations from −130 mV to a wide range of potentials. Under control conditions (■), the activation curve was well fit by a single Boltzmann function ($V_{1/2}$ = −57.3 mV, slope factor = e-fold/4.9 mV). Neither 10 (○) nor 50 μM (▼) verapamil significantly altered the activation curve ($V_{1/2}$ = −59.3 mV, slope factor = e-fold/5.5 mV and $V_{1/2}$ = −55.8 mV, slope factor = e-fold/5.2 mV, respectively), indicating that block was voltage-independent. Control, n = 11; 10 μM verapamil, n = 4; 50 μM verapamil, n = 3. Left inset, representative currents recorded under control conditions and in 10 μM verapamil. Right inset, representative I-V curves recorded under control conditions and in 10 and 50 μM verapamil. B, the use-dependent block of current by 10 μM verapamil was the same for voltage steps to −10 or +80 mV. Cells were repeatedly held at −130 mV for 100 ms and depolarized to either −10 or +80 mV for 100 ms (−10 mV, n = 4; +80 mV, n = 4). Representative currents in the absence and presence of 10 μM verapamil for depolarizations to either −10 or +80 mV are shown.

representative charge integrals for a single cell under control conditions and in the presence of 500 μM verapamil. The estimated verapamil IC_{50} value for I_{Ca} was probably less than 20 μM under these conditions; therefore, 500 μM was a saturating concentration sufficient to block greater than 96% of channels.

There were no discernible differences in the ON-gating currents or charge integrals between the control and drug conditions. For each cell, charge measured at each voltage was normalized to the maximum charge (Q_{max}) determined from the Boltzmann fit of the data. Charge versus voltage (Q-V) relationships normalized to the Q_{max} under control conditions (Fig. 9) demonstrate that verapamil did not change the amount of charge that was moved upon depolarization. Maximal charge was also unaffected when gating currents were measured in 500 μM verapamil in the absence of La^{3+} (data not shown). Fits from the Q-V relationships measured under control conditions yielded a voltage half-point ($V_{1/2}$) of -20 mV and a slope factor of e-fold/17.2 mV. The Q-V curve was shifted to potentials positive to those sufficient to elicit ionic current probably because of a substantial surface charge effect exerted by extracellular La^{3+}, a result consistent with previously published measurements of T-type Ca^{2+} channel gating currents (Lacinova et al., 2002; Lacinova and Klugbauer, 2004). Fitted parameters for the Q-V curve measured in the presence of verapamil were not statistically different from control ($V_{1/2}$ = -22 mV, slope factor = e-fold/19.6 mV), demonstrating that under these conditions, verapamil did not immobilize the voltage sensors and that drug-blocked channels gated normally.

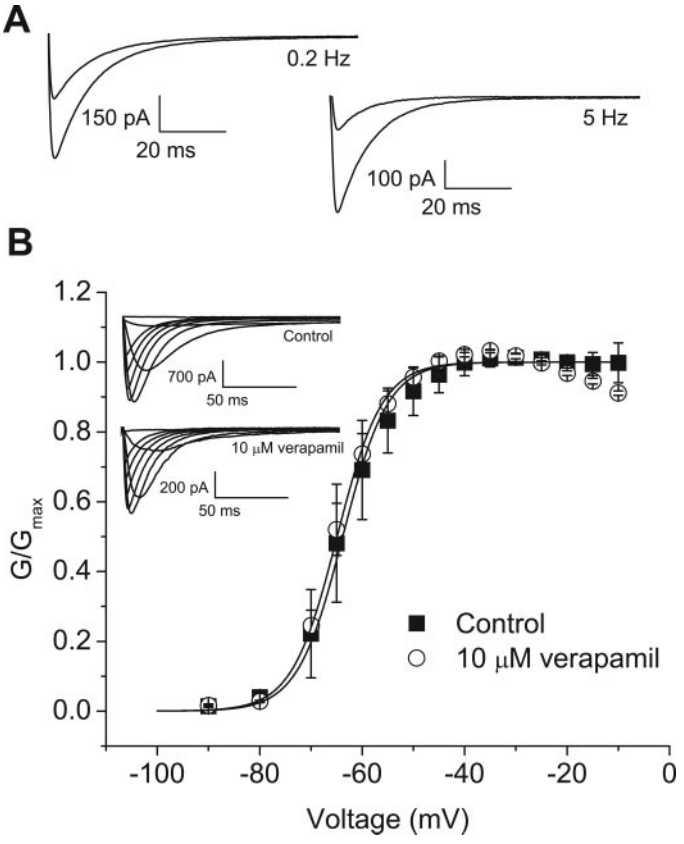

Fig. 8. The active form of verapamil was uncharged. A, at intracellular pH 6.1, 10 μM verapamil blocked 45% of peak current under 0.2-Hz stimulation, much less than expected if charged drug were the active species (n = 7). Under 5-Hz stimulation (n = 4), 10 μM verapamil blocked 72% of peak current, similar to the 68% inhibition at pH 7.4. Representative currents are shown for each stimulation frequency in the absence and presence of 10 μM verapamil. B, activation curves produced from 200-ms depolarizations from -130 mV at intracellular pH 6.1. Under control conditions (■), the G-V curve was well fit by a single Boltzmann function with $V_{1/2}$ = -63.8 mV and slope factor = e-fold/4.4 mV. In 10 μM verapamil (○), the activation curve had similar parameters ($V_{1/2}$ = -64.9 mV, slope factor = e-fold/4.4 mV). Control, n = 3; 10 μM verapamil, n = 4. Inset, representative currents for control and in 10 μM verapamil.

Discussion

T-type channels have been widely implicated in the control of vascular tone and blood pressure. Multiple studies have shown that T-channel inhibition is associated with the reduction of vascular smooth muscle tone in native tissues (Boulanger et al., 1994; Karila-Cohen et al., 1996; Lam et al., 1998; VanBavel et al., 2002; Jensen et al., 2004). T-channel blockade has been implicated in the successful treatment of hypertension. Mibefradil, a selective T-channel blocker (Mehrke et al., 1994; Mishra and Hermsmeyer, 1994; Clozel et al., 1997; Martin et al., 2000), exhibited favorable antihypertensive properties with minimal negative inotropic effects before its withdrawal from the market because of lethal drug interactions involving P450 cytochrome metabolism (Welker et al., 1998).

Two studies have challenged the notion that T-channel blockade promotes vasodilation. Chen et al. (2003) showed that $Ca_V3.2$ knockout mice paradoxically exhibited aberrant coronary arteriole constriction. Up-regulation of high-voltage-activated Ca^{2+} channels was probably not the cause of the constitutive vasoconstriction, but another compensatory mechanism may account for the unexpected $Ca_V3.2^{-/-}$ phenotype. More recently, Moosmang and colleagues (2003) generated a vascular smooth muscle-specific knockout of the $Ca_V1.2$ L-type channel, which they reported was unrespon-

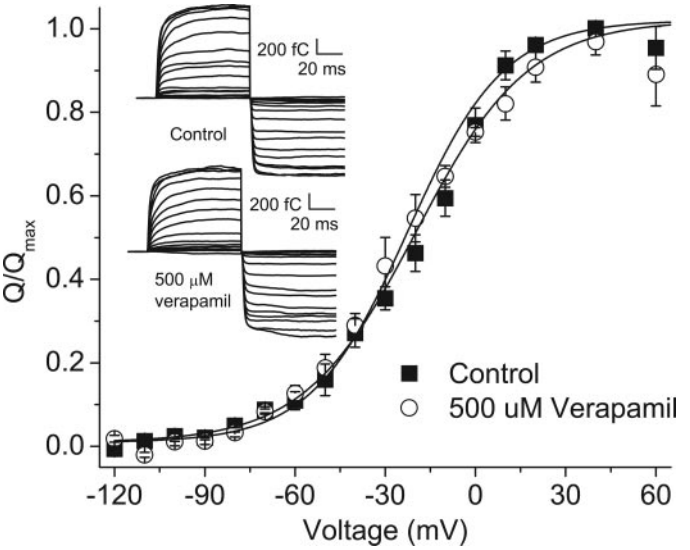

Fig. 9. Channels gated normally in the presence of drug. The Q-V curve measured under control conditions (■) (n = 3) was well fit by a single Boltzmann function with a $V_{1/2}$ of -20.3 mV and a slope factor of e-fold/17.2 mV. Fitted parameters for the Q-V curve measured in the presence of 500 μM verapamil (○) (n = 3) were not statistically different from control ($V_{1/2}$ = -22.4 mV, slope factor = e-fold/19.6 mV), demonstrating that verapamil did not alter gating charge movement. Ionic currents were blocked with 500 μM La^{3+}. Inset, representative charge integrals in the absence and presence of 500 μM verapamil.

sive to mibefradil (Moosmang et al., 2006). Although the authors concluded that mibefradil achieves its in vivo action by blocking $Ca_V1.2$, T channels are the preferential target in vitro (Boulanger et al., 1994; Karila-Cohen et al., 1996; Lam et al., 1998; VanBavel et al., 2002; Jensen et al., 2004). It may be that T channels modulate L-type channel-mediated calcium influx rather than directly controlling vascular tone. Because T channels open in response to small membrane depolarizations, their activation can further depolarize the membrane and promote L-channel activation and vasoconstriction. The lack of a mibefradil effect on $Ca_V1.2^{-/-}$ mice is consistent with this hypothesis, because T-channel modulation of L channels would have been ablated along with the L channel itself, even if the drug potently inhibited T channels.

Despite reports that verapamil is selective for L channels, our data demonstrate that it inhibits T-channel currents in the same concentration range needed to block heterologously expressed L-type channels (Motoike et al., 1999; Dilmac et al., 2004). The experimental manipulations necessary to separate T-type from L-type currents in native tissues may account for the reported disparities in drug affinity in these studies (Kuga et al., 1990). The ability of verapamil to inhibit both T-type and L-type channels in approximately the same concentration range suggests that blockade of both channels may contribute to its potent therapeutic effects, including blood pressure reduction and amelioration of reperfusion tachyarrhythmias (Kato et al., 2004) and paroxysmal supraventricular arrhythmias (Pritchett, 2004). Several studies have also suggested that block of L-type and T-type channels may contribute to effective control of electrical remodeling occurring with atrial fibrillation and tachycardia (Fareh et al., 1999, 2001; Ohashi et al., 2004).

Like other calcium channel blockers, verapamil blocks both L-type and T-type channels in a state-dependent manner (Nawrath and Wegener, 1997; Motoike et al., 1999; Heady et al., 2001; Dilmac et al., 2004). This feature is crucial from a clinical perspective, because the therapeutic effects of a drug are greatly influenced by the set of channel states that it preferentially targets. Clarifying the state-dependence of verapamil block of T channels is necessary to understand how verapamil achieves its in vivo effects, particularly because verapamil cross-reacts with multiple channel targets. In the present study, we used both whole-cell voltage-clamp and gating current measurements to systematically investigate the state-dependence of T-channel inhibition by verapamil. By expressing channels in HEK cells, we were able to study verapamil block of T-channels with minimal contamination by endogenous conductances, a significant obstacle in native tissues.

Using whole-cell voltage clamp, we showed that verapamil exhibited a moderate use-dependence and induced a dramatic slowing of recovery kinetics, features also observed in L channels (Johnson et al., 1996; Dilmac et al., 2004). The slow recovery kinetics indicate that verapamil is capable of inhibiting T channels over a time course much longer than that of the action potential, a feature which may be important in vivo. However, the lack of a substantial drug effect on the time course of T-channel currents suggests that the kinetics of inhibition are distinct from those observed for other channel targets. It is noteworthy that verapamil did not accelerate current decay as has been reported in L channels (Johnson et al., 1996; Dilmac et al., 2004) and K^+ channels (DeCoursey, 1995; Catacuzzeno et al., 1999; Robe and Grissmer, 2000); in addition, the drug unbinding reaction could not be observed in the tail currents (data not shown) as in K^+ channels (DeCoursey, 1995; Catacuzzeno et al., 1999; Robe and Grissmer, 2000).

The dependence on holding potential was strongly suggestive of high-affinity drug binding to an inactivated state of the channel. Consistent with that hypothesis, selective application of drug to inactivated channels produced a similar voltage dependence of block to that observed under equilibrium conditions. Because T-channels were substantially blocked by verapamil at potentials near the resting potential of vascular smooth muscle cells, this effect may be relevant to the drug's therapeutic profile. The finding that block was unaffected by the duration of short voltage steps (up to 50 ms) indicates that inactivated-state drug binding is significant only when channels dwell in this state for longer periods. It is plausible that inhibition of current during short voltage steps was due primarily to blockade of the open state of the channel, possibly followed by drug-induced conversion of the channel to a high-affinity-inactivated state.

The ability of verapamil to compete with both Ba^{2+} and Ca^{2+} implies that the binding site is located within the pore of the channel, as has been suggested for L-type channels and K^+ channels. Evidence that Ca^{2+} binds more tightly to the selectivity filter than Ba^{2+} does (Serrano et al., 2000) may explain the observation that verapamil more effectively competes with Ba^{2+} than with Ca^{2+}. It is noteworthy that block of L channels is more effective in Ca^{2+} than in Ba^{2+}, a phenomenon that may result from verapamil interaction with the Ca^{2+}-dependent inactivation process in these channels (Dilmac et al., 2004).

The observation that verapamil block was independent of the current-eliciting potential was unexpected but is consistent with results obtained for verapamil block of K^+ channels (DeCoursey, 1995; Robe and Grissmer, 2000). One possibility is that verapamil binds outside of the transmembrane electric field. However, when we selectively increased the cytoplasmic concentration of charged drug by lowering intracellular pH, drug block was not substantially enhanced. This finding suggested that the primary active species of drug was probably the uncharged form, which may bind within the field (in the pore) with no observable voltage-dependence. A similar mechanism has been proposed for verapamil inhibition of K^+ channels (DeCoursey, 1995; Catacuzzeno et al., 1999; Robe and Grissmer, 2000).

Voltage-dependent block of the open state at positive potentials would have been expected in single depolarizations if binding/unbinding were rapid or in trains of depolarizations if the interactions of the charged drug with the channel were slow. The absence of any such evidence argues against charged species blocking the open state. Likewise, the absence of a voltage-dependence of block at potentials positive to −70 mV during long depolarizations in which inactivated channels were selectively exposed to drug (Fig. 4D) also argues against the charged drug as the primary active species. Voltage-dependent partitioning of channels from closed states into inactivated states, rather than an interaction of the drug with the transmembrane field, probably accounts for the voltage-dependence of block observed at more negative potentials (Fig. 4, B and D).

The absence of a verapamil effect ON-gating currents and

charge suggests that it inhibits currents simply by occlusion of the conduction pathway. Stabilization of a channel conformation by an antagonist is usually accompanied by alteration of gating currents, as in the cases of lidocaine inhibition of Na^+ channels (Sheets and Hanck, 2003) and nifedipine inhibition of L-type Ca^{2+} channels (Hadley and Lederer, 1995). Because the T channel seems to gate normally, even in the presence of a saturating concentration of verapamil (500 μM), it is unlikely that the drug inhibits currents via a mechanism involving immobilization of the gating charge. However, it is possible that verapamil does allosterically stabilize a channel pore conformation in a manner that does not significantly affect voltage sensor movement.

Further work on the state-dependence of verapamil action, along with identification of high-affinity binding residues, are necessary steps toward understanding how phenylalkylamines modulate T-type channels in vivo. A complete understanding of how these important compounds affect T channels can refine the ways in which they are used clinically and guide the rational design of effective T-channel-selective drugs in the future.

Acknowledgments

We thank Constance Mlecko, John Kyle, J. R. Liu, and Katie Bittner for technical assistance.

References

Arnoult C, Villaz M, and Florman HM (1998) Pharmacological properties of the T-type Ca^{2+} current of mouse spermatogenic cells. *Mol Pharmacol* **53:**1104–1111.

Boulanger CM, Nakashima M, Olmos L, Joly G, and Vanhoutte PM (1994) Effects of the Ca^{2+} antagonist RO 40-5967 on endothelium-dependent responses of isolated arteries. *J Cardiovasc Pharmacol* **23:**869–876.

Budavari S (1996) *The Merck Index: an Encyclopedia of Chemicals, Drugs, and Biologicals.* Merck, Whitehouse Station, NJ.

Catacuzzeno L, Trequattrini C, Petris A, and Franciolini F (1999) Mechanism of verapamil block of a neuronal delayed rectifier K channel: active form of the blocker and location of its binding domain. *Br J Pharmacol* **126:**1699–1706.

Chen CC, Lamping KG, Nuno DW, Barresi R, Prouty SJ, Lavoie JL, Cribbs LL, England SK, Sigmund CD, Weiss RM, et al. (2003) Abnormal coronary function in mice deficient in alpha1H T-type Ca^{2+} channels. *Science (Wash DC)* **302:**1416–1418.

Clozel JP, Ertel EA, and Ertel SI (1997) Discovery and main pharmacological properties of mibefradil (Ro 40-5967), the first selective T-type calcium channel blocker. *J Hypertens Suppl* **15:**S17–S25.

DeCoursey TE (1995) Mechanism of K^+ channel block by verapamil and related compounds in rat alveolar epithelial cells. *J Gen Physiol* **106:**745–779.

Dilmac N, Hilliard N, and Hockerman GH (2004) Molecular determinants of frequency dependence and Ca^{2+} potentiation of verapamil block in the pore region of Cav1.2. *Mol Pharmacol* **66:**1236–1247.

Emerick MC, Stein R, Kunze R, McNulty MM, Regan MR, Hanck DA, and Agnew WS (2006) Profiling the array of $Ca_V3.1$ variants from the human T-type calcium channel gene *CACNA1G*: alternative structures, developmental expression, and biophysical variations. *Proteins* **64:**320–342.

Fareh S, Benardeau A, and Nattel S (2001) Differential efficacy of L- and T-type calcium channel blockers in preventing tachycardia-induced atrial remodeling in dogs. *Cardiovasc Res* **49:**762–770.

Fareh S, Benardeau A, Thibault B, and Nattel S (1999) The T-type Ca^{2+} channel blocker mibefradil prevents the development of a substrate for atrial fibrillation by tachycardia-induced atrial remodeling in dogs. *Circulation* **100:**2191–2197.

Fox AP, Nowycky MC, and Tsien RW (1987a) Kinetic and pharmacological properties distinguishing three types of calcium currents in chick sensory neurones. *J Physiol* **394:**149–172.

Fox AP, Nowycky MC, and Tsien RW (1987b) Single-channel recordings of three types of calcium channels in chick sensory neurones. *J Physiol* **394:**173–200.

Hadley RW and Lederer WJ (1995) Nifedipine inhibits movement of cardiac calcium channels through late, but not early, gating transitions. *Am J Physiol* **269:**H1784–H1790.

Heady TN, Gomora JC, Macdonald TL, and Perez-Reyes E (2001) Molecular pharmacology of T-type Ca^{2+} channels. *Jpn J Pharmacol* **85:**339–350.

Hering J, Feltz A, and Lambert RC (2004) Slow inactivation of the $Ca_V3.1$ isotype of T-type calcium channels. *J Physiol* **555:**331–344.

Hockerman GH, Johnson BD, Abbott MR, Scheuer T, and Catterall WA (1997) Molecular determinants of high affinity phenylalkylamine block of L-type calcium channels in transmembrane segment IIIS6 and the pore region of the α1 subunit. *J Biol Chem* **272:**18759–18765.

Hockerman GH, Johnson BD, Scheuer T, and Catterall WA (1995) Molecular determinants of high affinity phenylalkylamine block of L-type calcium channels. *J Biol Chem* **270:**22119–22122.

Jensen LJ, Salomonsson M, Jensen BL, and Holstein-Rathlou NH (2004) Depolarization-induced calcium influx in rat mesenteric small arterioles is mediated exclusively via mibefradil-sensitive calcium channels. *Br J Pharmacol* **142:**709–718.

Johnson BD, Hockerman GH, Scheuer T, and Catterall WA (1996) Distinct effects of mutations in transmembrane segment IVS6 on block of L-type calcium channels by structurally similar phenylalkylamines. *Mol Pharmacol* **50:**1388–1400.

Karila-Cohen D, Dubois-Rande JL, Giudicelli JF, and Berdeaux A (1996) Effects of mibefradil on large and small coronary arteries in conscious dogs: role of vascular endothelium. *J Cardiovasc Pharmacol* **28:**271–277.

Kato M, Dote K, Sasaki S, Takemoto H, Habara S, and Hasegawa D (2004) Intracoronary verapamil rapidly terminates reperfusion tachyarrhythmias in acute myocardial infarction. *Chest* **126:**702–708.

Kuga T, Sadoshima J, Tomoike H, Kanaide H, Akaike N, and Nakamura M (1990) Actions of Ca^{2+} antagonists on two types of Ca^{2+} channels in rat aorta smooth muscle cells in primary culture. *Circ Res* **67:**469–480.

Lacinova L and Klugbauer N (2004) Modulation of gating currents of the $Ca_V3.1$ calcium channel by alpha 2 delta 2 and gamma 5 subunits. *Arch Biochem Biophys* **425:**207–213.

Lacinova L, Klugbauer N, and Hofmann F (2002) Gating of the expressed Cav3.1 calcium channel. *FEBS Lett* **531:**235–240.

Lam E, Skarsgard P, and Laher I (1998) Inhibition of myogenic tone by mibefradil in rat cerebral arteries. *Eur J Pharmacol* **358:**165–168.

Martin RL, Lee JH, Cribbs LL, Perez-Reyes E, and Hanck DA (2000) Mibefradil block of cloned T-type calcium channels. *J Pharmacol Exp Ther* **295:**302–308.

Mehrke G, Zong XG, Flockerzi V, and Hofmann F (1994) The Ca^{++}-channel blocker Ro 40-5967 blocks differently T-type and L-type Ca^{++} channels. *J Pharmacol Exp Ther* **271:**1483–1488.

Mishra SK and Hermsmeyer K (1994) Selective inhibition of T-type Ca^{2+} channels by Ro 40-5967. *Circ Res* **75:**144–148.

Moosmang S, Haider N, Bruderl B, Welling A, and Hofmann F (2006) Antihypertensive effects of the putative T-type calcium channel antagonist mibefradil are mediated by the L-type calcium channel Cav1.2. *Circ Res* **98:**105–110.

Moosmang S, Schulla V, Welling A, Feil R, Feil S, Wegener JW, Hofmann F, and Klugbauer N (2003) Dominant role of smooth muscle L-type calcium channel Cav1.2 for blood pressure regulation. *EMBO (Eur Mol Biol Organ) J* **22:**6027–6034.

Motoike HK, Bodi I, Nakayama H, Schwartz A, and Varadi G (1999) A region in IVS5 of the human cardiac L-type calcium channel is required for the use-dependent block by phenylalkylamines and benzothiazepines. *J Biol Chem* **274:**9409–9420.

Nawrath H and Wegener JW (1997) Kinetics and state-dependent effects of verapamil on cardiac L-type calcium channels. *Naunyn-Schmiedeberg's Arch Pharmacol* **355:**79–86.

Ohashi N, Mitamura H, Tanimoto K, Fukuda Y, Kinebuchi O, Kurita Y, Shiroshita-Takeshita A, Miyoshi S, Hara M, Takatsuki S, et al. (2004) A comparison between calcium channel blocking drugs with different potencies for T- and L-type channels in preventing atrial electrical remodeling. *J Cardiovasc Pharmacol* **44:**386–392.

Perez-Reyes E (2003) Molecular physiology of low-voltage-activated t-type calcium channels. *Physiol Rev* **83:**117–161.

Perez-Reyes E, Cribbs LL, Daud A, Lacerda AE, Barclay J, Williamson MP, Fox M, Rees M, and Lee JH (1998) Molecular characterization of a neuronal low-voltage-activated T-type calcium channel. *Nature (Lond)* **391:**896–900.

Pritchett EL (2004) Symptomatic arrhythmia recurrence as an outcome in clinical trials of antiarrhythmic drug therapy. *Heart Rhythm* **1:**B36–B40.

Robe RJ and Grissmer S (2000) Block of the lymphocyte K^+ channel mKv1.3 by the phenylalkylamine verapamil: kinetic aspects of block and disruption of accumulation of block by a single point mutation. *Br J Pharmacol* **131:**1275–1284.

Serrano JR, Dashti SR, Perez-Reyes E, and Jones SW (2000) Mg^{2+} block unmasks Ca^{2+}/Ba^{2+} selectivity of alpha1G T-type calcium channels. *Biophys J* **79:**3052–3062.

Sheets MF and Hanck DA (2003) Molecular action of lidocaine on the voltage sensors of sodium channels. *J Gen Physiol* **121:**163–175.

VanBavel E, Sorop O, Andreasen D, Pfaffendorf M, and Jensen BL (2002) Role of T-type calcium channels in myogenic tone of skeletal muscle resistance arteries. *Am J Physiol* **283:**H2239–H2243.

Welker HA, Wiltshire H, and Bullingham R (1998) Clinical pharmacokinetics of mibefradil. *Clin Pharmacokinet* **35:**405–423.

Address correspondence to: Dr. Dorothy A. Hanck, 5841 South Maryland Avenue, MC 6094, Chicago, IL 60637. E-mail: dhanck@uchicago.edu